HHS Public Access

Author manuscript

Breast Cancer Res Treat. Author manuscript; available in PMC 2021 July 21.

Published in final edited form as:

Breast Cancer Res Treat. 2021 January ; 185(1): 1–12. doi:10.1007/s10549-020-05917-7.

Tumor necrosis by pretreatment breast MRI: association with neoadjuvant systemic therapy (NAST) response in triple-negative breast cancer (TNBC)

Abeer H. Abdelhafez[1], **Benjamin C. Musall**[2], **Beatriz E. Adrada**[1], **KennethR. Hess**[3], **Jong Bum Son**[2], **Ken-Pin Hwang**[2], **Rosalind P. Candelaria**[1], **Lumarie Santiago**[1], **Gary J. Whitman**[1], **Huong T. Le-Petross**[1], **Tanya W. Moseley**[1], **Elsa Arribas**[1], **Deanna L. Lane**[1], **Marion E. Scoggins**[1], **Jessica W. T. Leung**[1], **Hagar S. Mahmoud**[1], **Jason B. White**[4], **Elizabeth E. Ravenberg**[4], **Jennifer K. Litton**[4], **Vicente Valero**[4], **Peng Wei**[3], **Alastair M. Thompson**[5], **Stacy L. Moulder**[4], **Mark D. Pagel**[2,6], **Jingfei Ma**[2], **Wei T. Yang**[1], **Gaiane M. Rauch**[1,7]

[1]Department of Breast Imaging, The University of Texas MD Anderson Cancer Center, 1515 Holcombe Blvd., Unit 1350, Houston, TX 77030, USA

[2]Department of Imaging Physics, The University of Texas MD Anderson Cancer Center, 1515 Holcombe Blvd., Unit 1472, Houston, TX 77030, USA

[3]Department of Biostatistics, The University of Texas MD Anderson Cancer Center, 1515 Holcombe Blvd., Unit 1411, Houston, TX 77030, USA

[4]Department of Breast Medical Oncology, The University of Texas MD Anderson Cancer Center, 1515 Holcombe Blvd., Unit 1354, Houston, TX 77030, USA

[5]Department of Surgery, Baylor College of Medicine, 7200 Cambridge St., Houston, TX 77030, USA

[6]Department of Cancer Systems Imaging, The University of Texas MD Anderson Cancer Center, 1515 Holcombe Blvd., Unit 1907, Houston, TX 77030, USA

[7]Division of Diagnostic Imaging, Department of Abdominal Imaging, The University of Texas MD Anderson Cancer Center, 1515 Holcombe Blvd., Unit 1473, Houston, TX 77030, USA

Abstract

Purpose—To determine if tumor necrosis by pretreatment breast MRI and its quantitative imaging characteristics are associated with response to NAST in TNBC.

Methods—This retrospective study included 85 TNBC patients (mean age 51.8 ± 13 years) with MRI before NAST and definitive surgery during 2010–2018. Each MRI included T2-weighted, diffusion-weighted (DWI), and dynamic contrast-enhanced (DCE) imaging. For each index carcinoma, total tumor volume including necrosis (TTV), excluding necrosis (TV), and the necrosis-only volume (NV) were segmented on early-phase DCE subtractions and DWI images.

✉Gaiane M. Rauch, gmrauch@mdanderson.org.

Abeer H. Abdelhafez and Benjamin C. Musall have contributed equally to this work and share co-first authorship.

Wei T. Yang and Gaiane M. Rauch have contributed equally to this work and share co-last authorship.

NV and %NV were calculated. Percent enhancement on early and late phases of DCE and apparent diffusion coefficient were extracted from TTV, TV, and NV. Association between necrosis with pathological complete response (pCR) was assessed using odds ratio (OR). Multivariable analysis was used to evaluate the prognostic value of necrosis with T stage and nodal status at staging. Mann–Whitney *U* tests and area under the curve (AUC) were used to assess performance of imaging metrics for discriminating pCR vs non-pCR.

Results—Of 39 patients (46%) with necrosis, 17 had pCR and 22 did not. Necrosis was not associated with pCR (OR, 0.995; 95% confidence interval [CI] 0.4–2.3) and was not an independent prognostic factor when combined with T stage and nodal status at staging ($P = 0.46$). None of the imaging metrics differed significantly between pCR and non-pCR in patients with necrosis (AUC < 0.6 and $P > 0.40$).

Conclusion—No significant association was found between necrosis by pretreatment MRI or the quantitative imaging characteristics of tumor necrosis and response to NAST in TNBC.

Keywords

Triple-negative breast cancer; Multiparametric MRI; Necrosis; Diffusion-weighted MRI; Neoadjuvant therapy

Introduction

Triple-negative breast cancer (TNBC) accounts for approximately 20% of all breast cancers and is a subtype of breast cancer that lacks estrogen receptor, progesterone receptor, and HER2 expression [1]. Compared with other breast cancer subtypes, TNBC is more aggressive and is associated with a higher rate of relapse and a lower rate of overall survival [2, 3]. Patients with TNBC usually undergo neoadjuvant systemic therapy (NAST) for downstaging of disease to facilitate less invasive surgery. The extent of downstaging is used as a surrogate prognostic marker. Despite recent advances in breast cancer diagnosis and treatment, patients with TNBC tend to have a poor prognosis, with highly divergent response to treatment. Excellent response to NAST is seen in about half of the TNBC patients undergoing the treatment but weak or absent in the others [1, 2, 4].

Although still controversial, tumor necrosis detected at the histopathological evaluation has been proposed as a marker of poor prognosis in a variety of solid-organ malignancies [5]. A few studies have showed an association between tumor necrosis and poor treatment response and lower overall survival in colorectal and non-small cell lung cancer [6, 7]. However, such an association was not seen in renal cell carcinoma [8]. In breast cancer studies that included all hormonal subtypes, conflicting findings have been reported. One study showed that the presence of tumor necrosis correlated with tumor grade [9]. Two studies showed that the presence of tumor necrosis was associated with aggressiveness and unfavorable long-term outcomes [10, 11], while two other studies showed that the presence of tumor necrosis was associated with improved response to chemotherapy [12, 13]. Two additional studies showed no direct association between tumor necrosis and prognosis [14, 15].

Compared to other breast cancer subtypes, TNBC is more likely to display necrosis with a reported incidence ranging from 35 to 56% [16, 17]. The propensity for necrosis in TNBC

may be due to the tumor's aggressiveness (most TNBCs are of high grade) and increased mitotic activity (with high expression of proliferation marker Ki-67), characteristics that result in tumors outgrowing their blood supplies [18–21]. Tumor necrosis in TNBC has been evaluated on MR imaging in prior studies [2, 17, 22], as MRI can provide a comprehensive evaluation of the tumor and the accompanying necrosis on the basis of their often vastly different diffusion, perfusion and T2 relaxation characteristics. However, few studies have evaluated tumor necrosis in TNBC as an independent prognostic factor and predictor of response to NAST [2, 22]. In prior MRI-based studies of the association between tumor necrosis and tumor response to NAST, necrosis was assessed qualitatively based on a single slice of T2-weighted imaging [2, 22].

The objective of our study is to determine if tumor necrosis determined by pretreatment breast MRI and the quantitative imaging characteristics of tumor necrosis are associated with response to NAST in patients with TNBC.

Materials and methods

Patients

This retrospective study was conducted in compliance with the Health Insurance Portability and Accountability Act. Institutional Review Board approval was obtained and written informed consent was waived. A single institutional research database was searched to identify adult women (age ≥ 18 years) with pathologically proven stage I–III TNBC (ER, PR, HER2 negative) who underwent pretreatment breast MRI and NAST followed by definitive surgery during the period from April 2010 through December 2018 (Fig. 1).

MRI acquisition

All MRI studies were performed at our institution using MRI scanners that were approved for clinical breast MRI. These included 1.5T scanners (Signa HDxt and Optima MR450w, GE Healthcare Technologies, Waukesha, WI) and 3T scanners (Signa Discovery MR750w, GE Healthcare Technologies, Waukesha, WI; Magnetom Skyra, Siemens Health-ineers, Erlangen, Germany). All examinations were acquired with the patients in a prone position using dedicated eight-channel breast coils. The MRI protocol included bilateral axial non-contrast T1-weighted, axial fat-suppressed T2-weighted, pre-contrast axial diffusion-weighted imaging (DWI), axial dynamic contrast-enhanced (DCE) pre-contrast and post-contrast fat-suppressed T1-weighted, and delayed post-contrast sagittal fat-suppressed T1-weighted imaging.

DCE imaging was performed with the following parameters: temporal resolution, 90–120 s; total acquisition time, 6–8 min; repetition time, 6.0 ms; echo time, 2.0 ms; flip angle, 10°; slice thickness, 2.5 mm; and matrix, 256–480 × 256–324. Each patient received 0.1 mmol/kg gadobutrol (Gadovist, Bayer HealthCare) intravenously at a rate of 2 cc/s with a power injector. Serial subtraction images were generated during post-processing. Maps of percent enhancement (PE) relative to the mask series were calculated for the early phase (PE1) at approximately 60 s after injection and the delayed phase (PE2) at approximately 6 min after injection.

Typical scan parameters for DWI were as follows: echo time, 66 ms; repetition time, 7500 ms; flip angle, 90°; slice thickness, 5 mm; and matrix, 128 × 128. At least two *b*-values were used, with the lowest b-value ranging from 0 to 100 s/mm^2 and the highest *b*-value ranging from 800 to 1000 s/mm^2. Apparent diffusion coefficient (ADC) maps were calculated from DWI using a mono-exponential model.

MRI interpretation and segmentation

The largest lesion identified on DCE images was considered the index carcinoma and was used in our analysis. T stage was determined on the basis of the longest tumor dimension. Axillary lymph node status was assessed at staging by ultrasound-guided biopsy of suspicious lymph nodes and at surgery by pathologic review of the surgical specimen and was classified as positive or negative.

On the basis of the morphologic features on MRI, the index carcinomas were classified as necrotic or non-necrotic. Tumors were classified as necrotic if they displayed all three of the following features by visual assessment: a non-enhancing central or paracentral area on DCE images, hyperintensity of this central area on axial fat-suppressed T2-weighted images, and hyperintensity of this central area on ADC maps (Fig. 2).

Quantitative image analysis of necrotic carcinomas was performed with ImageI, an image visualization and processing software developed in-house. ImageI was used for tumor contouring and analyses of a previously published work on esophageal cancer [23]. Among many commonly useful utilities, ImageI offers convenient DICOM image import from the patient PACS system, customizable model fitting of the images, graphical user interface-based manual and semi-automatic tumor segmentation and contouring, and easy export of the tumor ROI statistics and quantitative metrics including different radiomics features.

Two breast radiologists, both with at least 5 years of experience in breast MRI interpretation, were blinded to the patient outcome data and performed segmentation encompassing the tumor in all slices. Segmentations were further refined using the histogram thresholding in ImageI to exclude voxels that were visually determined to be non-tumor by the radiologist. These segmentations were performed separately on both early DCE subtractions and ADC maps. All segmentations were reviewed and confirmed by both radiologists to avoid inter-reader bias. The segmented regions were the total tumor volume including necrosis (TTV), the tumor volume excluding necrosis (TV), and the necrosis-only volume (NV) (Fig. 3).

For DCE, TV_{DCE} was manually defined as the fraction of the TTV_{DCE} with visual enhancement, which was assumed to correspond to viable tumor. The $\%NV_{DCE}$ was calculated from the extracted volumes as:

$$\%NV_{DCE} = 100\% \times \frac{NV_{DCE}}{NV_{DCE} + TV_{DCE}} \quad (1)$$

PE1 and PE2 were calculated from voxel signal levels as:

$$PE1 = 100\% \times \frac{S_{\text{early phase}} - S_{\text{mask phase}}}{S_{\text{mask phase}}} \quad (2)$$

$$PE2 = 100\% \times \frac{S_{\text{delayed phase}} - S_{\text{mask phase}}}{S_{\text{mask phase}}} \quad (3)$$

where S is the signal level for each respective phase. Average PE1 and PE2 values were extracted from the tumor ROIs as determined on the early-phase DCE images for TTV_{DCE}, TV_{DCE}, and NV_{DCE}.

On DWI, viable tumor tissue was visually identified as areas of restricted diffusion that displayed high signal intensity on high b-value images (i.e., 800 or 1000) with a corresponding low ADC signal intensity. The mean ADC values from TTV_{DWI}, TV_{DWI}, and NV_{DWI} segmentations were calculated. The quantitative ADC analysis was performed on subset of patients with necrotic carcinomas after exclusion of DW images with large clip artifact or DWI performed after contrast administration which may introduced error in ADC value assessment. However, all DW images were available for visual assessment for presence or absence of necrosis.

Response assessment

Patients were dichotomized into pathologic complete response (pCR) and non-pCR groups on the basis of findings from surgical histopathology. pCR was defined as absence of residual invasive cancer with or without ductal carcinoma in situ in the breast and the absence of carcinoma in the sampled axillary lymph nodes.

Statistical analysis

A statistical association of the imaging parameters assessed on DCE imaging and ADC maps relative to pCR was performed using the statistics module in Matlab (version 2018b, Mathworks, Natick, MA). An odds ratio (OR) analysis was used to determine the value of necrosis as a predictor of response to NAST. Association of necrosis with T stage and nodal status was assessed using chi-square test and OR, respectively. Separately, multiple logistic regression, using R Statistical Software (Foundation for Statistical Computing, Vienna, Austria), was used to create a model for predicting pCR with the following variables: presence of necrosis, T stage, and pretreatment axillary lymph node status. Mann–Whitney U test and the area under the receiver operator characteristic curve (AUC) were used to compare image metrics between the pCR and non-pCR groups. Finally, we performed power analyses to assess the power of our comparisons between measurements and pCR status. P-values less than 0.05 were considered statistically significant. No correction was made for multiple comparisons.

Results

Patient characteristics

A total of 85 women met the selection criteria and were included in the study (Fig. 1). Patient and tumor characteristics of these 85 women are presented in Table 1. The mean, median, and range of the patient age in years at diagnosis were 51.8 ± 13, 51, 26–78, respectively. The median longest tumor diameter measured at DCE imaging was 3.8 cm (range 1.3–9.8 cm).

Regarding NAST, 76/85 (89%) of the 85 patients received standard chemotherapy consisting of doxorubicin and cyclophosphamide followed by paclitaxel, and 9/85 (11%) patients received a combination of doxorubicin and cyclophosphamide followed by paclitaxel and then followed by targeted therapy. The median number of cycles received was 6 (range 4–8). Of the 85 patients, 47/85 (55%) underwent total mastectomy, and 38/85 (45%) underwent segmentectomy.

Thirty-seven patients 37/85 (44%) had pCR, and 48/85 (56%) did not; 39/85 (46%) patients had necrotic tumors and 46/85 (54%) patients had non-necrotic tumors (Table 2). Of 39 patients with necrotic carcinoma, 17/39 (44%) had pCR (Fig. 4), and 22/39 (56%) did not (Fig. 5).

Association of necrosis with T stage, axillary nodal status, and pCR

The frequency of tumor necrosis in the 85 patients with TNBC based on T stage, nodal status at staging and at surgery, and pCR are provided in Table 2. The likelihood of necrosis increased with increasing T stage (X^2 (2, N = 85) = 5.321, P = 0.070). No association was observed between the presence of necrosis and nodal status at staging (OR 1.19; 95% confidence interval [CI] 0.5–2.8) or nodal status at surgery (OR 0.850; 95% CI 0.3–2.3).

There was no association between the presence of necrosis and pCR (OR 0.995; 95% CI 0.4–2.3). Multiple logistic regression to predict pCR based on the presence of necrosis, T stage, and nodal status at staging showed that necrosis was not a significant independent prognostic factor of pCR status (P = 0.46, Table 3).

Association of DCE imaging metrics with pCR in necrotic TNBC subset

The mean NV_{DCE} was 5.9 cm^3 (SD ± 6.8 cm^3) for the pCR group and 7.7 cm^3 (SD ± 10.8 cm^3) for the non-pCR group. The mean $\%NV_{DCE}$ was 14% (SD ± 12%) for the pCR group and 14% (SD ± 10.4%) for the non-pCR group (Fig. 6). There was no significant difference in the NV_{DCE} (AUC = 0.58; P = 0.37) and %NV (AUC = 0.50; P = 0.90) between the two groups.

Among the necrotic index carcinomas, there were no differences between the pCR and non-pCR groups in PE1 and PE2 of the TTV_{DCE}, TV_{DCE}, or NV_{DCE} (Table 4). At a significance level of 0.05, we can have 80% power to detect an AUC of ≥ 0.75.

Association of DWI imaging metrics with pCR in necrotic TNBC subset

For quantitative evaluation of necrotic regions on DWI, 22/39 (56%) necrotic tumors in the study were included. The remaining 17 necrotic tumors were excluded for quantitative assessment of ADC value because the DWI showed severe clip-related metallic artifact or DWI were acquired after contrast agent administration, also were available for visual assessment for presence of necrosis. Of the 22 patients with necrotic index carcinomas and available for quantitative evaluation of ADC, 8/22 (36%) had pCR and 14/22 (64%) did not.

There were no differences between the pCR and non-pCR groups in the mean ADC for the TTV_{DWI}, TV_{DWI} or NV_{DWI} for necrotic tumors (Table 4). At a significance level of 0.05, we can have 80% power to detect an AUC of ≥ 0.84.

Discussion

Our study did not find significant association between the presence of tumor necrosis by pretreatment MRI and response to NAST in patients with TNBC. In patients with necrotic index carcinomas, the necrosis-only volume, necrosis as a percent of the TTV, and quantitative perfusion and diffusion metrics were not significantly different between the patients with and without a pCR.

Tumor necrosis detected at histopathological evaluation has been investigated in multiple studies for different types of carcinomas and has been proposed as a poor prognostic factor in a variety of solid tumors, as it is thought to reflect chronic hypoxia and poor vascularity [5, 7, 8, 24]. Previous studies based on the review of pathological specimens have reported conflicting results regarding the association between tumor necrosis and overall survival in breast cancer. One study showed that tumor necrosis correlated with tumor grade, but did not compare necrosis directly with outcome [9]. Two studies showed that tumor necrosis was associated with poor clinical outcomes and aggressive tumor biology, as well as decreased relapse-free survival and increased mortality [10, 11]. In an analysis of over 1200 patients with HER2-positive tumors, necrosis was not associated with overall survival, although necrotic tumors represented only 9% of selected patients [25]. In another cohort of 1850 patients of different hormonal subtypes, necrosis was associated with tumor characteristics suggesting poor outcome and was an independent adverse prognostic factor for disease-free survival [3]. It should be noted that in the aforementioned studies, necrosis rates were between 4.5% and 9%, which were substantially lower than those reported in other studies with a necrosis rate of up to 40% among different hormonal subtypes [5]. Some other studies do not demonstrate a clear correlation between tumor necrosis and prognosis in breast cancer [14, 15].

A few studies have specifically evaluated the association between tumor necrosis seen at histopathological evaluation and prognostic outcomes in patients with TNBC. In a study of 154 patients with TNBC that examined age, clinical stage, Ki-67 proliferation index, tumor necrosis, lymph node status, and histological grade, tumor necrosis was found by univariate analyses to be a significant negative prognostic factor of relapse-free survival [26]. A second study of 149 patients with TNBC showed better disease-free survival for smaller tumor size (≤ 2 cm) and absence of necrosis based on univariate analysis. However, a multivariable

analysis of the same data revealed no statistically significant association between necrosis and disease-free survival [27]. A third study of 87 TNBCs showed that pathologic characteristics, including necrosis, were not associated with overall prognosis [21]. In a cohort of 841 TNBCs, tumor necrosis was associated with mortality but was not a prognostic factor for recurrence [16].

Very few MRI-based studies have investigated whether necrosis predicts response of TNBC to NAST. In a study of 23 patients with TNBC, Kawashima et al. [22] sought to differentiate responders from non-responders to NAST and found that irregularly shaped mass and the presence of clear intratumoral necrosis were significantly associated with absence of response. However, 5 patients (21%) had necrotic index carcinomas in this study, which was substantially lower than the number and percentage of patients with necrotic carcinomas in our study (39 /46%), and is lower than the typical reported rate of necrosis of up to 50% in TNBCs [16]. More importantly, the response assessment in this study was based on response evaluation criteria in solid tumors (RECIST) rather than the pathological response at surgery, which is a generally accepted as a potential surrogate marker for survival in TNBC [28]. In another study of 132 patients with TNBC, Bae et al. [2] examined the association between pretreatment breast MRI features and pCR and recurrence-free survival and found that the absence of intratumoral T2 high signal intensity, representing necrosis, was associated with pCR. However, this association was not statistically significant. Furthermore, only 18 of the 132 patients (13%) had a pCR, which is substantially lower than the 44% rate of pCR seen in our study as well as the typical range of 33% to 45% among TNBC patients as reported by others [29–32]. In comparison, our study population was more representative of the typical TNBC population in terms of their rates of pCR and necrosis. Further, our analysis included evaluation of quantitative imaging characteristics of necrosis in addition to the qualitative assessment of the presence of necrosis. One plausible hypothesis explaining the similar outcomes between necrotic and non-necrotic tumors observed in our study is that tissue hypoxia at the necrotic core may result in increased local angiogenic growth factors, making the tumor more aggressive but also more vulnerable to treatment due to improved perfusion and drug delivery. However, further work is needed to investigate this hypothesis and other possible physiological changes in necrotic and non-necrotic tumors.

To the best of our knowledge, the association between necrotic carcinoma and nodal disease in TNBC has not been investigated. In our study, we found that necrosis was not significantly associated with nodal disease either at staging or at surgical pathology.

Our study differs from prior studies of necrosis on MRI as a predictive marker in TNBC in that we conducted a comprehensive quantitative analysis of tumors with and without necrosis as well as the necrotic region itself, on both DCE images and diffusion-weighted images, and tested association between these quantitative imaging metrics with pCR after NAST. In our analysis, we also focused on necrosis as an independent predictor of treatment response and investigated the behavior of the solid and necrotic components of necrotic tumors both separately and in combination. In comparison, all the prior studies were based mainly on binary evaluation of presence or absence of necrosis on T2-weighted images.

Our study had several limitations. First, this is a retrospective study performed in a single institution with a relatively small patient population. Second, the segmentation of the different tissue volumes was performed by two breast radiologists in consensus, and we did not evaluate inter-observer variability in segmentation. Third, while all DWI images were available for visual assessment for presence or absence of necrosis, the quantitative ADC analysis was performed on a subgroup of necrotic lesions due to technical limitations. Finally, the NAST treatment protocols in our study population were heterogeneous as they depended on clinician preference, yet this heterogeneity reflects the adaptive design that is used in actual clinical practice for best patient outcome.

In conclusion, our study did not find significant associations between tumor necrosis by pretreatment MRI and the quantitative image characteristics of tumor necrosis and the response to NAST in TNBC patients. Our findings warrant further validation in larger population-based multi-institutional studies that evaluate not only response to NAST but also long-term outcomes.

Acknowledgements

We would like to thank Stephanie P. Deming from the Department of Scientific Publications, Research Medical Library, at The University of Texas MD Anderson Cancer Center for her assistance in editing and proofreading this document.

Funding

This study has received funding by the National Institutes of Health/National Cancer Institute (Cancer Center Support Grant P30 CA016672); specifically resources from the Biostatistics Resource Group were used.

Conflict of interest

Dr. Ken-Pin Hwang receives research funding from GE Healthcare; Dr. Tanya W. Moseley is an imaging consultant for Hologic Inc. and Merit Medical Inc.; Dr. Elsa Arribas is a shareholder and serves on the advisory board for Volumetric, Inc.; Dr. Jessica W.T. Leung is an advisor for Subtle Imaging and CureMetrix, and is a speaker for Fujifilm; Dr. Jingfei Ma has ongoing financial relationships with GE Healthcare, Siemens Healthcare, and C4 Imaging; Dr. Mark D. Pagel receives research funding from BioInVision, Inc., and Roche Pharma; receives research benefits from iThera Medical, Inc., Phantech, Inc., and PhotoSound, Inc.; and has a financial relationship with Genentech, Inc.; Dr. Wei T. Yang receives royalties from Elsevier; Dr. Gaiane M. Rauch receives research funding from GE Healthcare.

Abbreviations

ADC	Apparent diffusion coefficient
DCE	DYNAMIC contrast enhanced
DWI	Diffusion-weighted imaging
NAST	Neoadjuvant systemic therapy
NV	Necrosis volume
pCR	Pathological complete response
PE	Percent enhancement
TNBC	Triple-negative breast cancer

TTV	Total tumor volume
TV	Tumor volume without necrosis

References

1. Bao C, Lu Y, Chen J, Chen D, Lou W, Ding B, Xu L, Fan W (2019) Exploring specific prognostic biomarkers in triple-negative breast cancer. Cell Death Dis 10(11):807 [PubMed: 31649243]
2. Bae MS, Shin SU, Ryu HS, Han W, Im SA, Park IA, Noh DY, Moon WK (2016) Pretreatment mr imaging features of triple-negative breast cancer: association with response to neoadjuvant chemotherapy and recurrence-free survival. Radiology 281(2):392–400 [PubMed: 27195438]
3. Maiorano E, Regan MM, Viale G, Mastropasqua MG, Colleoni M, Castiglione-Gertsch M, Price KN, Gelber RD, Goldhirsch A, Coates AS (2010) Prognostic and predictive impact of central necrosis and fibrosis in early breast cancer: Results from two international breast cancer study group randomized trials of chemoendocrine adjuvant therapy. Breast Cancer Res Treat 121(1):211–218 [PubMed: 19280340]
4. Bauer KR, Brown M, Cress RD, Parise CA, Caggiano V (2007) Descriptive analysis of estrogen receptor (er)-negative, progesterone receptor (pr)-negative, and her2-negative invasive breast cancer, the so-called triple-negative phenotype. Cancer 109(9):1721–1728 [PubMed: 17387718]
5. Richards CH, Mohammed Z, Qayyum T, Horgan PG, McMillan DC (2011) The prognostic value of histological tumor necrosis in solid organ malignant disease: a systematic review. Future Oncol 7(10):1223–1235 [PubMed: 21992733]
6. Vayrynen SA, Vayrynen JP, Klintrup K, Makela J, Karttunen TJ, Tuomisto A, Makinen MJ (2016) Clinical impact and network of determinants of tumour necrosis in colorectal cancer. Br J Cancer 114(12):1334–1342 [PubMed: 27195424]
7. Fujisaki A, Aoki T, Kasai T, Kinoshita S, Tomoda Y, Tanaka F, Yatera K, Mukae H, Korogi Y (2016) Pleomorphic carcinoma of the lung: Relationship between ct findings and prognosis. AJR Am J Roentgenol 207(2):289–294 [PubMed: 27144416]
8. Zhang L, Zha Z, Qu W, Zhao H, Yuan J, Feng Y, Wu B (2018) Tumor necrosis as a prognostic variable for the clinical outcome in patients with renal cell carcinoma: a systematic review and meta-analysis. BMC Cancer 18(1):870 [PubMed: 30176824]
9. Dietzel M, Baltzer PA, Vag T, Herzog A, Gajda M, Camara O, Kaiser WA (2010) The necrosis sign in magnetic resonance-mammography: diagnostic accuracy in 1,084 histologically verified breast lesions. Breast J 16(6):603–608 [PubMed: 21070437]
10. Jimenez RE, Wallis T, Visscher DW (2001) Centrally necrotizing carcinomas of the breast: a distinct histologic subtype with aggressive clinical behavior. Am J Surg Pathol 25(3):331–337 [PubMed: 11224603]
11. Zhang Y, Ou Y, Yu D, Yong X, Wang X, Zhu B, Zhang Q, Zhou L, Cai Z, Cheng Z (2015) Clinicopathological study of centrally necrotizing carcinoma of the breast. BMC Cancer 15:282 [PubMed: 25880163]
12. Pu RT, Schott AF, Sturtz DE, Griffith KA, Kleer CG (2005) Pathologic features of breast cancer associated with complete response to neoadjuvant chemotherapy: importance of tumor necrosis. Am J Surg Pathol 29(3):354–358 [PubMed: 15725804]
13. Masood S (2016) Neoadjuvant chemotherapy in breast cancers. Womens Health (Lond) 12(5):480–491 [PubMed: 27885165]
14. Lee AH, Gillett CE, Ryder K, Fentiman IS, Miles DW, Millis RR (2006) Different patterns of inflammation and prognosis in invasive carcinoma of the breast. Histopathology 48(6):692–701 [PubMed: 16681685]
15. Kato T, Kimura T, Miyakawa R, Tanaka S, Fujii A, Yamamoto K, Kameoka S, Hamano K, Kawakami M, Aiba M (1997) Clinicopathologic study of angiogenesis in japanese patients with breast cancer. World J Surg 21(1):49–56 [PubMed: 8943177]
16. Urru SAM, Gallus S, Bosetti C, Moi T, Medda R, Sollai E, Murgia A, Sanges F, Pira G, Manca A, Palmas D, Floris M, Asunis AM, Atzori F, Carru C, D'Incalci M, Ghiani M, Marras V, Onnis D, Santona MC, Sarobba G, Valle E, Canu L, Cossu S, Bulfone A, Rocca PC, De Miglio MR, Orru S

(2018) Clinical and pathological factors influencing survival in a large cohort of triple-negative breast cancer patients. BMC Cancer 18(1):56 [PubMed: 29310602]

17. Uematsu T, Kasami M, Yuen S (2009) Triple-negative breast cancer: correlation between mr imaging and pathologic findings. Radiology 250(3):638–647 [PubMed: 19244039]
18. Keam B, Im SA, Lee KH, Han SW, Oh DY, Kim JH, Lee SH, Han W, Kim DW, Kim TY, Park IA, Noh DY, Heo DS, Bang YJ (2011) Ki-67 can be used for further classification of triple negative breast cancer into two subtypes with different response and prognosis. Breast Cancer Res 13(2):R22 [PubMed: 21366896]
19. Walsh EM, Keane MM, Wink DA, Callagy G, Glynn SA (2016) Review of triple negative breast cancer and the impact of inducible nitric oxide synthase on tumor biology and patient outcomes. Crit Rev Oncog 21(5–6):333–351 [PubMed: 29431082]
20. Fulford LG, Easton DF, Reis-Filho JS, Sofronis A, Gillett CE, Lakhani SR, Hanby A (2006) Specific morphological features predictive for the basal phenotype in grade 3 invasive ductal carcinoma of breast. Histopathology 49(1):22–34 [PubMed: 16842243]
21. Ryu DW, Jung MJ, Choi WS, Lee CH (2011) Clinical significance of morphologic characteristics in triple negative breast cancer. J Korean Surg Soc 80(5):301–306 [PubMed: 22066052]
22. Kawashima H, Inokuchi M, Furukawa H, Kitamura S (2011) Triple-negative breast cancer: are the imaging findings different between responders and nonresponders to neoadjuvant chemo-therapy? Acad Radiol 18(8):963–969 [PubMed: 21652233]
23. Fang P, Musall BC, Son JB, Moreno AC, Hobbs BP, Carter BW, Fellman BM, Mawlawi O, Ma J, Lin SH (2018) Multimodal imaging of pathologic response to chemoradiation in esophageal cancer. Int J Radiat Oncol Biol Phys 102(4):996–1001 [PubMed: 29685377]
24. Collins J, Epstein JI (2017) Prognostic significance of extensive necrosis in renal cell carcinoma. Hum Pathol 66:108–114 [PubMed: 28669641]
25. Rilke F, Colnaghi MI, Cascinelli N, Andreola S, Baldini MT, Bufalino R, Della Porta G, Menard S, Pierotti MA, Testori A (1991) Prognostic significance of her-2/neu expression in breast cancer and its relationship to other prognostic factors. Int J Cancer 49(1):44–49 [PubMed: 1678734]
26. Liu YX, Wang KR, Xing H, Zhai XJ, Wang LP, Wang W (2016) Attempt towards a novel classification of triple-negative breast cancer using immunohistochemical markers. Oncol Lett 12(2):1240–1256 [PubMed: 27446423]
27. Pistelli M, Pagliacci A, Battelli N, Santinelli A, Biscotti T, Ballatore Z, Berardi R, Cascinu S (2013) Prognostic factors in early-stage triple-negative breast cancer: lessons and limits from clinical practice. Anticancer Res 33(6):2737–2742 [PubMed: 23749934]
28. Cortazar P, Zhang L, Untch M, Mehta K, Costantino JP, Wolmark N, Bonnefoi H, Cameron D, Gianni L, Valagussa P, Swain SM, Prowell T, Loibl S, Wickerham DL, Bogaerts J, Baselga J, Perou C, Blumenthal G, Blohmer J, Mamounas EP, Bergh J, Semiglazov V, Justice R, Eidtmann H, Paik S, Piccart M, Sridhara R, Fasching PA, Slaets L, Tang S, Gerber B, Geyer CE Jr, Pazdur R, Ditsch N, Rastogi P, Eiermann W, von Minckwitz G (2014) Pathological complete response and long-term clinical benefit in breast cancer: the ctneobc pooled analysis. Lancet 384(9938):164–172 [PubMed: 24529560]
29. Hudis CA, Barlow WE, Costantino JP, Gray RJ, Pritchard KI, Chapman JA, Sparano JA, Hunsberger S, Enos RA, Gelber RD, Zujewski JA (2007) Proposal for standardized definitions for efficacy end points in adjuvant breast cancer trials: the steep system. J Clin Oncol 25(15):2127–2132 [PubMed: 17513820]
30. Moulder S, Moroney J, Helgason T, Wheler J, Booser D, Albarracin C, Morrow PK, Koenig K, Kurzrock R (2011) Responses to liposomal doxorubicin, bevacizumab, and temsirolimus in metaplastic carcinoma of the breast: biologic rationale and implications for stem-cell research in breast cancer. J Clin Oncol 29(19):e572–575 [PubMed: 21482991]
31. Houssami N, Macaskill P, von Minckwitz G, Marinovich ML, Mamounas E (2012) Meta-analysis of the association of breast cancer subtype and pathologic complete response to neoadjuvant chemotherapy. Eur J Cancer 48(18):3342–3354 [PubMed: 22766518]
32. Sharma P, Lopez-Tarruella S, Garcia-Saenz JA, Khan QJ, Gomez HL, Prat A, Moreno F, Jerez-Gilarranz Y, Barnadas A, Picor-nell AC, Monte-Millan MD, Gonzalez-Rivera M, Massarrah T, Pelaez-Lorenzo B, Palomero MI, Gonzalez Del Val R, Cortes J, Fuentes-Rivera H, Morales DB,

Marquez-Rodas I, Perou CM, Lehn C, Wang YY, Klemp JR, Mammen JV, Wagner JL, Amin AL, O'Dea AP, Heldstab J, Jensen RA, Kimler BF, Godwin AK, Martin M (2018) Pathological response and survival in triple-negative breast cancer following neoadjuvant carboplatin plus docetaxel. Clin Cancer Res 24(23):5820–5829 [PubMed: 30061361]

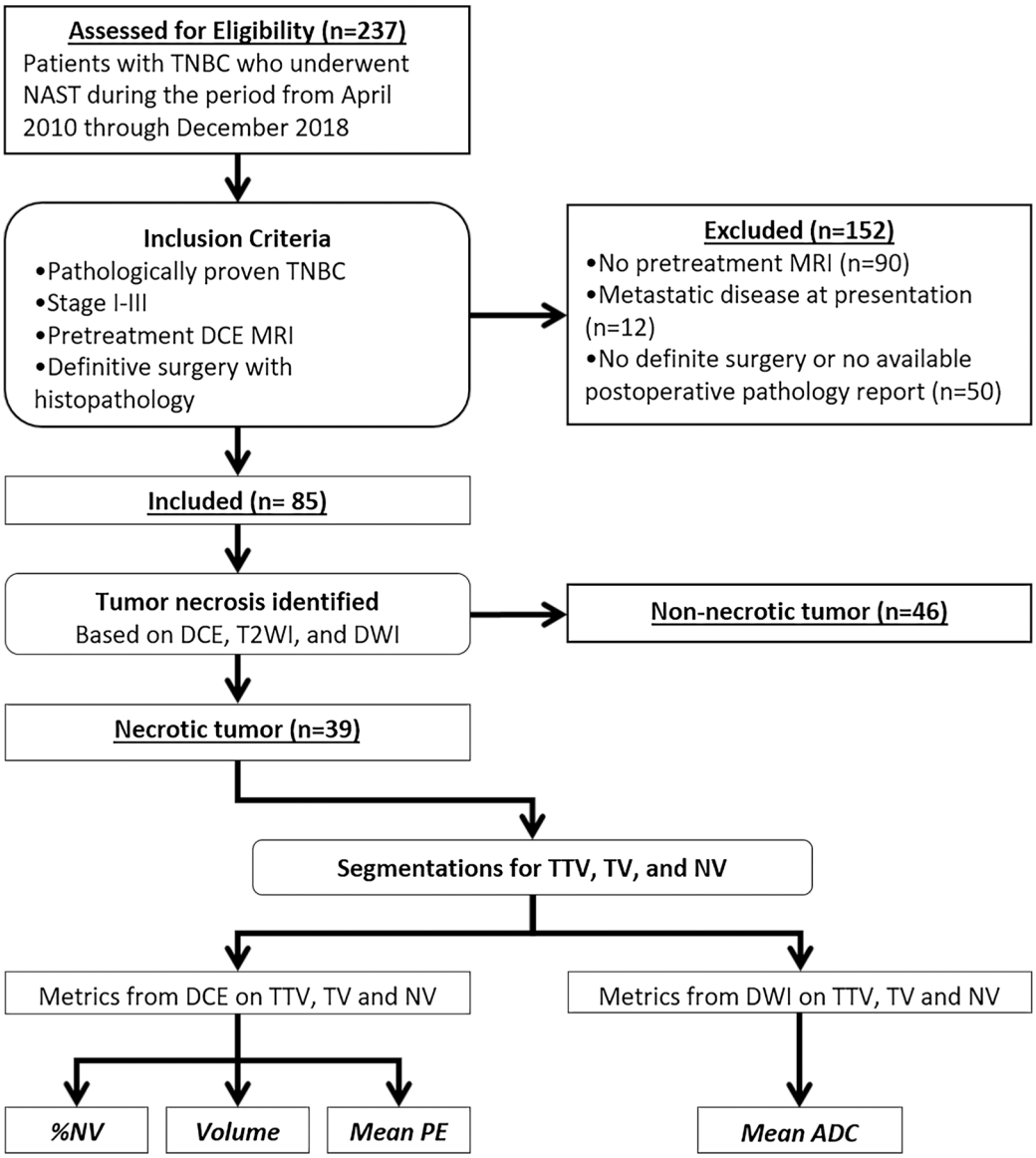

Fig. 1.

Inclusion criteria and assignment of analysis for each group. *ADC* apparent diffusion coefficient, *DCE* dynamic contrast-enhanced imaging, *DWI* diffusion-weighted imaging, *NAST* neoadjuvant systemic therapy, *NV* necrosis-only volume, *PE* percent enhancement, *T2WI* T2-weighted imaging, *TNBC* triple-negative breast cancer, *TTV* total tumor volume including necrosis, *TV* tumor volume without necrosis

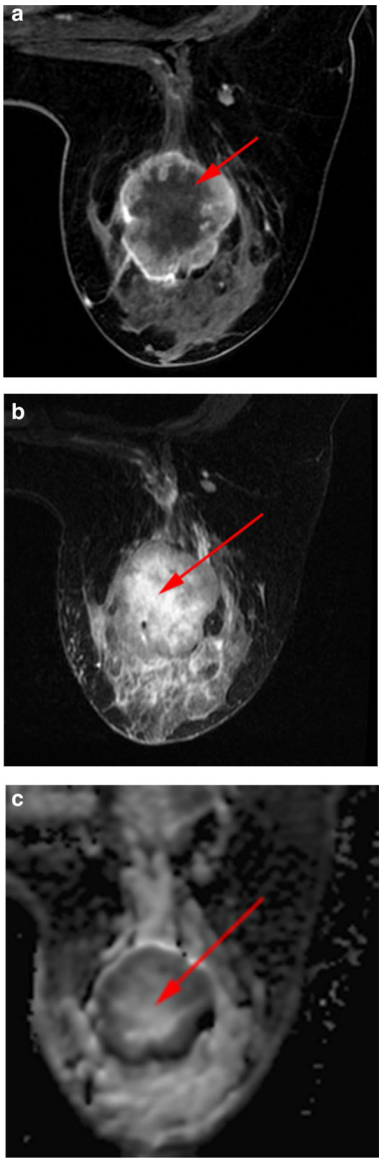

Fig. 2.

Necrosis in a 35-year-old woman with TNBC of the left breast. **a** Axial fat-suppressed early-phase dynamic contrast-enhanced image shows central non-enhancing area representing necrosis (arrow). **b** Axial fat-suppressed T2-weighted image shows necrosis as central area of high signal intensity (arrow). **c** Axial apparent diffusion coefficient map shows shine-through corresponding to central area of necrosis (arrow) seen on dynamic contrast-enhanced and T2-weighted imaging

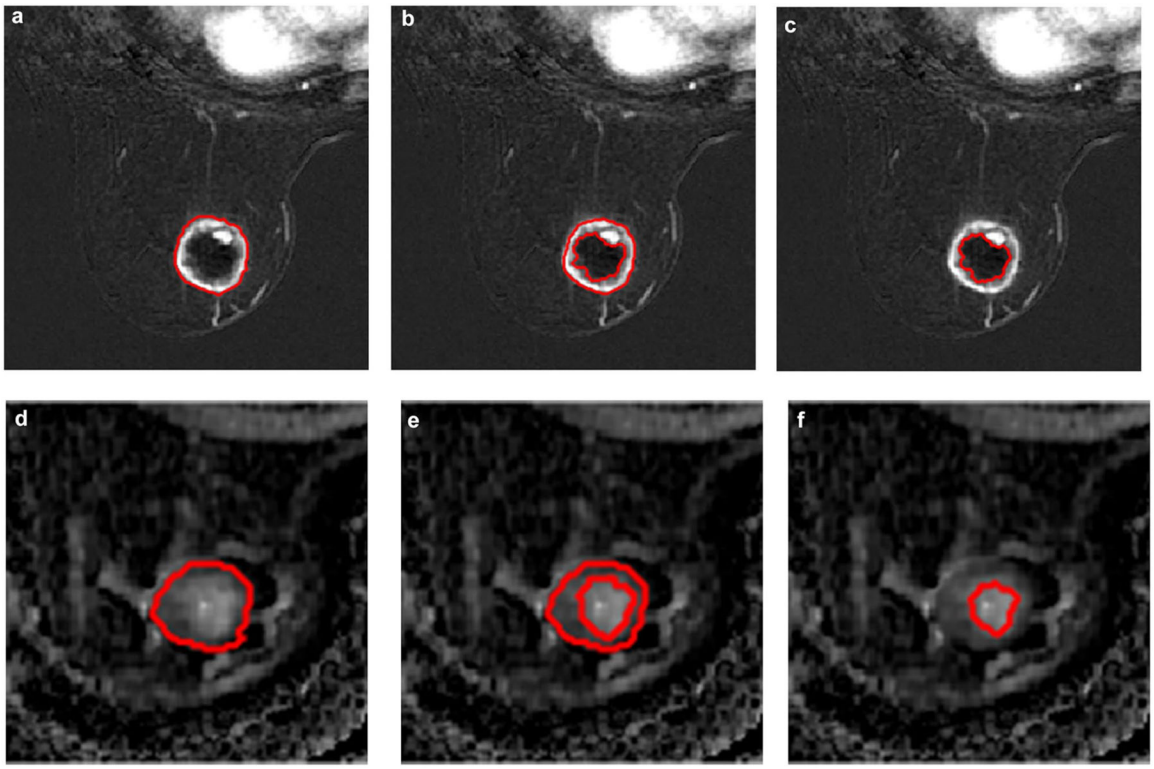

Fig. 3.

Segmentation technique in a 60-year-old woman with TNBC of the right breast. Axial dynamic contrast-enhanced early-phase fat-suppressed images with whole tumor (**a**), tumor without necrosis (**b**), and necrosis-only (**c**) segmentations, as well as corresponding apparent diffusion coefficient maps (**d**, **e**, **f**)

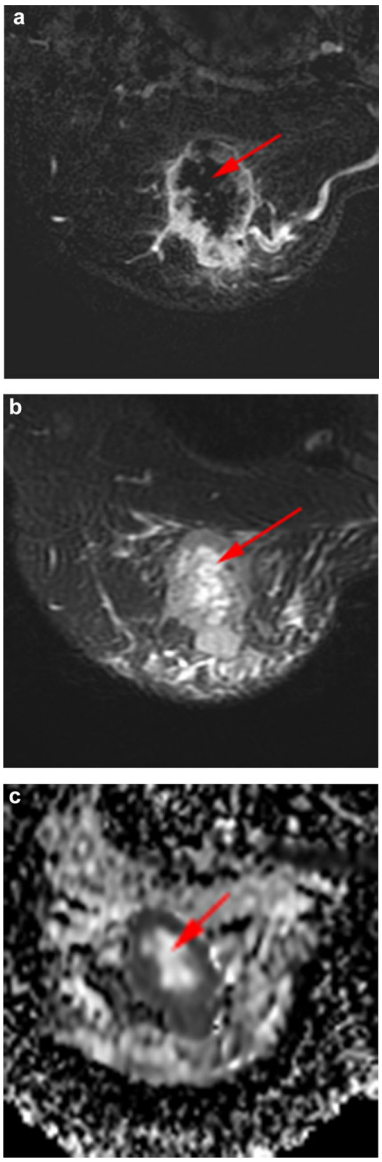

Fig. 4.

Necrotic index carcinoma with a pathological complete response after neoadjuvant systemic therapy in a 46-year-old woman with TNBC of the right breast. The volume of necrotic material was 10 cm^3, and the percent of the total tumor volume occupied by necrosis was 17%. **a** Axial fat-suppressed early-phase dynamic contrast-enhanced image shows central non-enhancing area representing necrosis (arrow). **b** Axial fat-suppressed T2-weighted image shows necrosis as central area of high signal intensity (arrow). **c** Axial apparent diffusion coefficient map shows shine-through corresponding to the central area of necrosis (arrow)

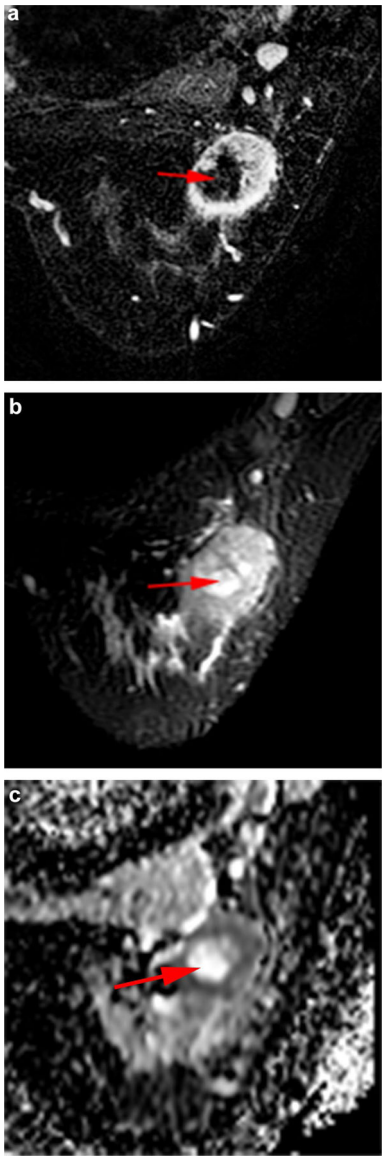

Fig. 5.

Necrotic index carcinoma with pathological non-complete response after neoadjuvant systemic therapy in a 30-year-old woman with TNBC of the left breast. The volume of necrotic material was 4 cm^3, and the percent of the total tumor volume occupied by necrosis was 17%. **a** Axial fat-suppressed early-phase dynamic contrast-enhanced image shows central non-enhancing area representing necrosis (arrow). **b** Axial fat-suppressed T2-weighted image shows necrosis as a central area of high signal intensity (arrow). **c** Axial apparent diffusion coefficient map shows shine-through corresponding to central area of necrosis (arrow)

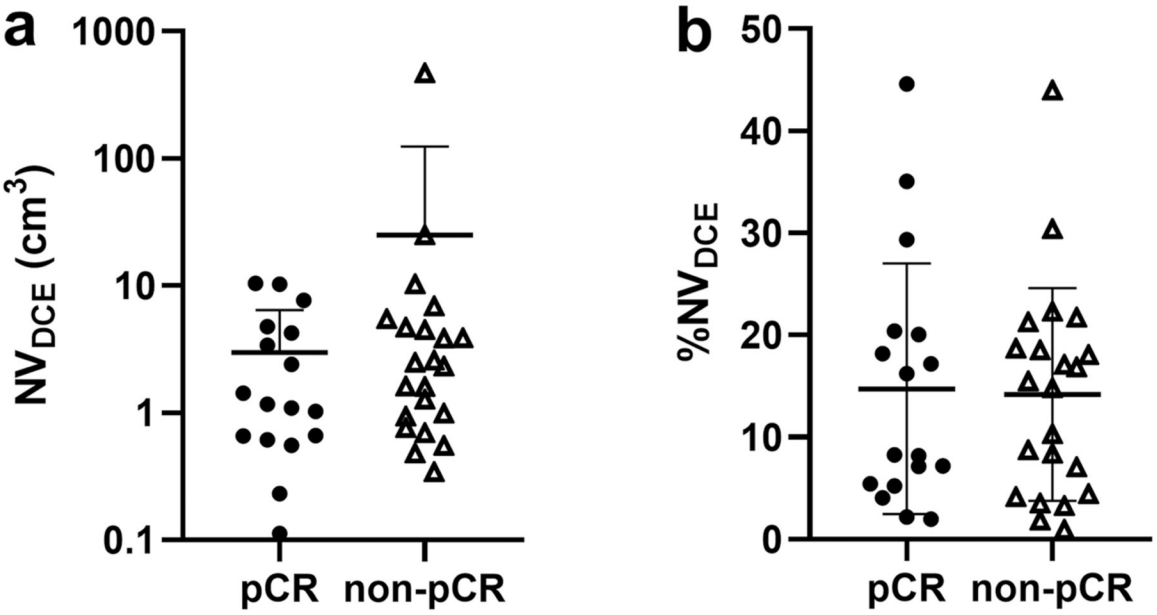

Fig. 6.

Clustering of necrosis volume or NV_{DCE} (**a**) and necrosis-only volume as a percent of total tumor volume or $\%NV_{DCE}$ (**b**), by dynamic contrast-enhanced MRI associated with response to neoadjuvant systemic therapy. There is no difference between TNBC patients with and without pathologic complete response (pCR)

Table 1

Characteristics of 85 patients with triple-negative breast cancer who received neoadjuvant systemic therapy

Characteristic	Study population	pCR	Non-pCR
No. of patients	85	37/85 (44)	48/85 (56)
Age (years)			
Mean ± SD	51.8 ± 13	54.3 ± 13.8	49.9 ± 12.39
Median (range)	51 (26–78)	57 (27–78)	47 (26–75)
Longest tumor diameter (cm)			
Mean ± SD	4.57 ± 2.9	3.6 ± 2.18	5.3 ± 3.3
Median (range)	3.8 (1.3–9.8)	3 (1.3–4.4)	4.25 (1.6–9.8)
Tumor histological type			
IDC grade II	10/85 (12)	2/37 (5)	8/48 (17)
IDC grade III	72/85 (85)	35/37 (95)	37/48 (77)
Metaplastic	3/85 (3)	0/37 (0)	3/48 (6)
Necrotic tumor histological type			
IDC grade II	5/85 (6)	1/37 (3)	4/48 (8)
IDC grade III	32/85 (38)	16/37 (43)	16/48 (33)
Metaplastic	2/85 (2)	0/37 (0)	2/48 (4)
Tumor classification on DCE imaging			
Non-necrotic (solid)	46/85 (54)	20/37 (54)	26/48 (54)
Necrotic	39/85 (46)	17/37 (46)	22/48 (46)
Type of surgery			
Total mastectomy	47/85 (55)	21/37 (57)	28/48 (58)
Conservative surgery	38/85 (45)	16/37 (43)	20/48 (42)

Data are number of patients (percent) unless otherwise indicated

DCE dynamic contrast-enhanced, *IDC* infiltrating ductal carcinoma, pCR pathological complete response, *SD* standard deviation, *TNBC* triple-negative breast cancer

Table 2

T stage, nodal status, and pathologic complete response in 85 triple-negative breast cancer patients and the subsets of patients with or without necrotic carcinomas

Characteristic	Study population (*n* = 85)	Necrotic carcinomas (*n* = 39)	Non-necrotic carcinomas (*n* = 46)	*P*-value
T stage				0.07
T1	14/85 (16)	3/39 (8)	11/46 (24)	
T2	44/85 (52)	20/39 (51)	24/46 (52)	
T3	27/85 (32)	16/39 (41)	11/46 (24)	
Nodal status at staging				0.69
Positive	46/85 (54)	22/39 (56)	24/46 (52)	
Negative	39/85 (46)	17/39 (44)	22/46 (48)	
Nodal status at surgery				0.75
Positive	21/85 (25)	9/39 (23)	12/46 (26)	
Negative	64/85 (75)	30/39 (77)	34/46 (74)	
pCR status				0.99
pCR	37/85 (44)	17/39 (44)	20/46 (43)	
Non-pCR	48/85 (56)	22/39 (56)	26/46 (57)	

Data are number of patients (percent) with the exception of the *P*-value column. *P*-values comparing characteristic distributions between necrotic and non-necrotic patients used Chi-square test

pCR pathological complete response

Table 3

Logistic regression results for association analysis of pCR with presence of necrosis, T stage, and pretreatment nodal stage

Parameter	β	Standard error	*z*-statistic	*P*-value	Exp(β) (adjusted odds ratio)
Necrosis	0.36	0.49	0.74	0.46	1.44
T stage (2)	− 0.64	0.65	− 0.98	0.33	0.53
T stage (3)	− 1.88	0.77	− 2.45	0.014	0.15
Nodal stage	− 0.63	0.47	− 1.34	0.18	0.53

Table 4

DCE and DWI metrics from whole tumor, tumor without necrosis, and necrosis-only segmentations of necrotic carcinomas

Metric	pCR	Non-pCR	AUC	*P*-value
DCE (*n* = 39)	*n* = 17/39 (44%)	*n* = 22/39 (56%)		
NV_{DCE} (cm^3)	5.9 ± 6.8	7.7 ± 10.8	0.59	.37
$\%NV_{DCE}$	14 ± 12	14 ± 10.4	0.50	.99
PE1 TTV_{DCE}	189.2 ± 26	164.37 ± 58	0.51	.97
PE2 TTV_{DCE}	102 ± 12	183.77 ± 51	0.52	.83
PE1 TV_{DCE}	213.17 ± 30.42	184.8 ± 56	0.51	.97
PE2 TV_{DCE}	220.7 ± 14.8	202.6 ± 57	0.53	.77
PE1 NV_{DCE}	58.37 ± 45	64.45 ± 95	0.52	.81
PE2 NV_{DCE}	106.37 ± 67	133.35 ± 97	0.55	.62
DWI (*n* = 22)	*n* = 8/22 (36%)	*n* = 14/22 (64%)		
ADC TTV_{DWI} (10^{-3} mm^2/s)	1.26 ± 0.36	1.20 ± 0.22	0.53	.83
ADC TV_{DWI} (10^{-3} mm^2/s)	1.08 ± 0.23	1.13 ± 0.26	0.51	.97
ADC NV_{DWI} (10^{-3} mm^2/s)	1 ± 0.5	1.7 ± 0.3	0.53	.87

Data are mean ± standard deviation unless otherwise indicated

ADC apparent diffusion coefficient, *AUC* area under the receiver operating characteristics curve, *DCE* dynamic contrast-enhanced, *DWI* diffusion-weighted imaging, *pCR* pathological complete response, *NV* volume of necrosis, *%NV* percent of necrosis, *PE1* percent enhancement at early phase, *PE2* percent enhancement at delayed phase, *TTV* total tumor volume including necrosis, *TV* tumor volume excluding necrosis